PFC/RR/82-9

DOE/ET/51013-37
UC20F

OBSERVATION OF THE PARAMETRIC DECAY INSTABILITY DURING ELECTRON CYCLOTRON RESONANCE HEATING ON THE VERSATOR II TOKAMAK

F.S. McDermott, G. Bekefi, and M. Porkolab
Department of Physics and
Research Laboratory of Electronics
Massachusetts Institute of Technology
Cambridge, Massachusetts 02139

March 1982

This work is supported by DOE Contract DE-AC02-78ET-51013.

OBSERVATION OF THE PARAMETRIC DECAY INSTABILITY DURING ELECTRON CYCLOTRON RESONANCE HEATING ON THE VERSATOR II TOKAMAK

F.S. McDermott, G. Bekefi, and M. Porkolab

Department of Physics and Research Laboratory of Electronics

Massachusetts Institute of Technology

Cambridge, Massachusetts 02139

ABSTRACT

Observations are reported on a nonlinear, three wave interaction process occurring during high power electron cyclotron heating in the Versator II tokamak. The measured spectra and the threshold power are consistent with a model in which the incident power in the extraordinary mode of polarization decays at the upper-hybrid resonance layer into a lower-hybrid wave and an electron Bernstein wave.

Parametric instabilities caused by large amplitude electric fields with frequencies near the electron cyclotron frequency are important in understanding RF heating[1] of plasmas. In particular, such instabilities may occur during injection perpendicular to the magnetic field or in pre-ionization and startup experiments. Several studies[2] have been made of parametric wave instabilities in tenuous, low temperature media. Here we report the observation of parametric decay effects in a dense, hot, toroidal plasma. Similar parametric processes may have occured in other tokamak experiments[1,3] and bumpy tori.[4] The observed spectra and the measured threshold power for the parametric decay are consistent with a model in which the incident RF power in the extraordinary mode of polarization decays into a lower-hybrid and an electron Bernstein mode. The wave coupling is taken to occur in a plasma layer where the frequency of the pump wave equals approximately to the upper-hybrid frequency. Parametric decay near the upper-hybrid frequency has been observed in recent computer simulations.[5] However, in such computer simulations the threshold has been derived under the assumption of a uniform plasma. Recent theoretical calculations predict that inhomogeneities may significantly raise the threshold power for parametric excitation,[6,7] which is in agreement with our observations.

The experiments were carried out on the Massachusetts Institute of Technology Versator II tokamak:[8] R_0=40cm; a_L=13cm; I_{OH}=50 kA; t(pulse)=30msec; $\bar{n}_e=(2\times10^{12})-(1\times10^{13})\,cm^{-3}$; T_{e0}=200-350eV; T_{i0}=100-160eV; $Z_{eff}\simeq2$; B(toroidal)=12.5kG. The RF power source is the Naval Research Laboratory 35.08GHz gyrotron[9] capable of providing up to 150kW of power with a 10msec pulse length, excellent

frequency stability, and narrow spectral width ($\Delta\omega/\omega \simeq 10^{-4}$). Figure 1 illustrates the experimental arrangement. The circularly polarized electromagnetic wave emanating from the gyrotron is guided by a circular waveguide in the TE_{01} mode; it is then converted into a linearly polarized TE_{11} mode of a circular waveguide and finally injected into the tokamak from inside the torus. Thus, the waveguide terminates on the high magnetic field side of the toroidal field where a reflecting mirror directs the power toward the central region of the plasma. The antenna pattern can be approximated by a pencil-beam having a full width at the half power points of $\sim 20°$. The mirror is hinged so that the angle of incidence, θ, relative to the normal to the magnetic field, can be varied from $-40° < \theta < +40°$ (positive angles denote injection along the direction of the plasma current and negative angles denote injection counter to the plasma current). In all the experiments reported here, $\theta = +20°$, and the electric vector of the incident wave is polarized almost[10] parallel to the direction that corresponds to the extraordinary wave polarization in the plasma. We note that when the polarization is rotated so as to correspond to the ordinary plasma mode, no parametric decay instabilities are seen. In all the work reported here, the toroidal magnetic field is adjusted so as to place the electron cyclotron resonance on the geometric axis of the torus.

In order to observe the higher frequency decay wave in the three-wave coupling process, a Ka band (35GHz) microwave superheterodyne receiver is connected to a horn antenna (Fig. 1). An Impatt diode serves as a local oscillator and is tuned to the gyrotron output frequency ($\omega_0/2\pi = 35.08$GHz). Although the local oscil-

lator has a tendency to drift up to 10MHz during the course of experimentation, the drift is much less than the width of the detected spectrum. The output of the mixer is displayed directly on a spectrum analyzer. A waveguide stop-band filter, (see Fig. 1) placed between the plasma and the mixer apparatus, protects the sensitive electronics from excessive power at the gyrotron frequency. Its frequency characteristics are sufficiently narrow so as not to perturb the measured spectrum. The Ka band receiving horn is located on the low magnetic field side of the torus directly opposite the RF output window, in the $\theta=0$ plane. The low-frequency wave is observed by means of an electrostatic probe connected directly to a spectrum analyzer. Due to the high plasma temperatures in Versator, the probe must be positioned at the edge of the plasma, near the limiter radius.

Typical photographs of the spectrum analyzer output for the Ka band detector are shown in Fig. 2. In Fig. 2a we frequency sweep the spectrum analyzer during the RF injection. The detected wave spectrum centered at a frequency of approximately 400MHz away from the gyrotron frequency, $\omega_0/2\pi$, is clearly evident. The broadening about the reference frequency is due to the width of the Impatt local oscillator. If the local oscillator is not tuned to exactly the gyrotron frequency but is mismatched by $\Delta\omega$, a third resonance would appear at the mismatch frequency. In this way, the frequency tuning can be continuously monitored. In Fig. 2b, we do not frequency sweep the spectrum analyzer but instead monitor the time-history of the emission at a difference frequency of 425MHz. We see that the emission remains roughly constant during the course of the RF injection.

Figures 3a and 3b illustrate the spectra measured with the Ka band detector and with the electrostatic probe, respectively, for a gyrotron power of 120kW incident on a plasma with a line-average density, $\bar{n}_e = 0.5 \times 10^{13} cm^{-3}$. We see that the Ka band signal has a frequency separation, $(\omega_0 - \omega_1)/2\pi$, from the gyrotron frequency of 400MHz, which is just equal to the measured frequency, $\omega_2/2\pi = 400MHz$ on the electrostatic probe. Thus, the frequency matching condition, $\omega_0 = \omega_1 + \omega_2$, characteristic of three-wave parametric decay processes, is satisfied. We also observe in Fig. 3b a resonance at 800MHz which appears to be a second harmonic of ω_2. It is not known whether this resonance is a wave from the bulk of the plasma or if it is generated[11] in the sheath of the probe. We shall not concern ourselves further with this resonance.

The intensity of the decay wave is a strong function of the gyrotron (pump wave) incident power. This is illustrated in Fig. 4 for two values of plasma number density. In both cases we observe a threshold power level of approximately 50kW for the pump wave below which parametric decay does not occur. There is a tendency to have somewhat lower thresholds at lower densities (see Fig. 4).

We assume[12] that the three wave interaction described above occurs near the upper-hybrid frequency $\omega_{UH} = (\omega_{pe}^2 + \omega_{ce}^2)^{1/2}$ as is illustrated in Fig. 1, (ω_{pe} and ω_{ce} are the electron plasma and electron cyclotron frequencies respectively) since in this layer the electric field of the pump wave is predicted[5,13] to be largest. The two decay waves, namely the electron Bernstein mode of frequency ω_1 and the lower-hybrid mode of frequency ω_2, are taken to propagate perpendicular to the toroidal magnetic field

so that the parallel wave numbers $k_{1\parallel}$ and $k_{2\parallel}$ are approximately equal to zero. Under these conditions the dispersion relations of the two modes, for a plasma with a Maxwellian distribution of velocities, are given by

$$\omega_1^2 = \omega_{UH}^2 - \omega_{pe}^2 b_1 \tag{1}$$

$$\omega_2^2 = \omega_{LH}^2 \left[1 + (3b_2\omega_{ce}\omega_{ci}T_i)/(\omega_2^2 T_e)\right] \tag{2}$$

where $b_1=k_{1\perp}^2 r_{ce}^2$, $b_2=k_{2\perp}^2 r_{ce}^2$ and $k_{1\perp}, k_{2\perp}$ are the wave numbers perpendicular to the magnetic field; $r_{ce}=(T_e/m)^{1/2}\omega_{ce}^{-1}$ is the electron gyroradius and T_e is the electron temperature; $\omega_{LH} = \omega_{pi}\left(1 + \omega_{pe}^2/\omega_{ce}^2\right)^{-1/2}$ is the lower-hybrid frequency; and ω_{ci} and T_i are the ion cyclotron frequency and temperature, respectively. In writing these equations we have assumed that $\omega_{pe}^2 \lesssim \omega_{ce}^2$ and $b_{1,2} \ll 1$. If, moreover, one goes to the dipole limit[6] $k_0 \to 0$, it follows from the selection rule $\vec{k}_0=\vec{k}_1+\vec{k}_2$ that $k_{1\perp}=-k_{2\perp}\equiv k_\perp$ and thus, $b_1=b_2\equiv b$. Making use of Eqs. (1) and (2) in conjunction with the frequency selection rule $\omega_0=\omega_1+\omega_2$, we obtain the sought-after quantities b, ω_{pe}, and $\omega_2/k_\perp v_{th,i}\left(v_{th,i}=(T_i/M)^{1/2}\right)$ to be used in calculating the threshold for the parametric instability. From the experimentally determined values of $\omega_0/2\pi=35.08$GHz, $\omega_2/2\pi=400$GHz, $T_e/T_i\simeq 2$, we obtain, $b\simeq 0.14$, $\omega_{pe}/2\pi\simeq 14.3\text{GHz}\left(n_e\simeq 0.26\times 10^{13}\text{cm}^{-3}\right)$, $\omega_{ce}/2\pi\simeq 32.0$GHz(B=11.4kG), and $\omega_2/k_\perp v_{th,i}\simeq 1$. From these values of n_e and B, and from the (approximately) known radial profiles of the plasma density and of the toroidal magnetic field, one can estimate the positions on the upper-hybrid curve (Fig. 1) along which the parametric wave processes occurs. Our results indicate that the interaction takes place in the outer layers of the plasma. This may explain why the apparently heavily Landau damped lower-hybrid "quasi-mode"[7]

$(\omega_2/k_\perp v_{th,i} \simeq 1)$ does not lead to ion heating in the parameter range of this experiment: in these outer regions of the plasma, confinement of energetic ions is poor.

For the case of a homogeneous plasma, the threshold for decay into an electron Bernstein wave and damped lower-hybrid quasi-mode is given by the expression,[7]

$$\frac{(E_x)^2_{th}}{64\pi n_e T_e} = \frac{\nu_{coll}}{\omega_1}\left(\frac{\omega_0^2 + \omega_{ce}^2}{\omega_{ce}^2}\right)\frac{1}{4b} \qquad (3)$$

where $(E_x)_{th}$ is the threshold electric field strength for decay and ν_{coll} is the electron-ion collision frequency. Substituting our previous estimates and the values of $T_e \simeq 100$eV and $\nu_{coll} \simeq 1\times10^5$ sec^{-1}, we find, $(E_x)_{th} \simeq 0.39$ esu or 115V/cm. Modeling the inhomogeneous case, we shall now calculate the convective threshold. Here, wave growth occurs in a region in front of the ω_{UH} layer whose width Δx is approximately equal to the density gradient scale length.[13] Assuming that in this interaction region the threshold growth rate is much larger than any of the damping rate terms for the lower sideband, the threshold for decay is given by[7]

$$\frac{(E_x)^2_{th}}{64\pi n_e T_e} = \frac{1}{4}\frac{\omega_{pe}^2}{\omega_{ce}^2}\left(\frac{2\pi}{k_\perp \Delta x}\right) \qquad (4)$$

Substituting our previous numerical results in the above equation and assuming $\Delta x = 1.5$cm, we find $(E_x)_{th} \simeq 10$ esu or 3000V/cm. Estimates of the effective field strength enhancement[5,13] occurring in the extraordinary mode dispersion relation at the upper-hybrid resonance give $(E_x/E_y)_{UH} \simeq 5$, and the threshold electromagnetic power flux becomes $P_{th} = (c/8\pi)(E_y)^2_{th}$, or 500W/cm^2. The antenna illumi-

nates an area of the upper-hybrid layer of approximately $100cm^2$ yielding a threshold incident power level $\simeq 50kW$. This is in reasonable agreement with the results of Fig. 4, since in Versator single pass absorption of the extraordinary mode at the cyclotron resonance is at most 30%. On the other hand, the homogeneous plasma approximation based on Eq. (3) gives a threshold power level $\simeq 75Watts$, almost three orders of magnitude below the measured value.

In conclusion, we have observed radiation from both decay products of a nonlinear, three-wave coupling process occurring during electron cyclotron resonance heating of the Versator II tokamak. Our measurements are consistent with extraordinary mode coupling at the upper-hybrid resonance to a lower-hybrid wave and an electron Bernstein mode. Theoretical estimates are in reasonable agreement with the experimentally observed threshold if inhomogeneities and WKB enhancement of the incident electromagnetic fields are properly accounted for. Homogeneous plasma theory gives a threshold which is some three orders in magnitude below the experimentally observed value. Our model predicts that the lower-hybrid decay wave is resonant with the ions. Based on recent lower-hybrid heating experiments[14] this may result in the formation of an energetic ion tail. In larger machines or different magnetic field geometries, this tail may be well confined and collisional transfer of energy to the bulk ions occurs. Furthermore, the effects of small but finite values of $k_{\parallel}$ (due to pump wave beam width and/or magnetic shear) could damp the Berstein mode after it has propagated from the upper-hybrid interaction region back to the electron cyclotron resonance where it could be

absorbed by electrons near the center of the plasma column.[13] In this way, at high RF input powers the parametric decay process may lead to additional heating and thus increase the overall efficiency compared to that predicted by single-pass cyclotron absorption theories.[13] Such processes may be particularly important in small tokamaks and in electron cyclotron preionization and startup experiments.

ACKNOWLEDGMENTS

This work was supported by the United States Department of Energy (Contract DE-AC02-78ET-51013).

We gratefully acknowledge the support of the members of the Versator research group and engineering staff. In particular, K.E. Hackett who designed the waveguide filter and NRL staff J.S. Levine and M.E. Read who have provided the gyrotron.

REFERENCES

1. R.M. Gilgenbach, M.E. Read, K.E. Hackett, R. Lucey, B. Hui, V.L. Granatstein, K.R. Chu, A.C. England, C.M. Loring, O.C. Eldridge, H.C. Howe, A.G. Kulchar, E. Lazarus, M. Murakami, and J.B. Wilgen, Phys. Rev. Lett. 44:10, 647 (1980); C.P. Moeller, V.S. Chan, A. Funahashi, K. Hoshino, R.J. La Haye, R. Prater, T. Yamamoto, and T. Yamauchi, General Atomic Report GA-A16397 (1981); R.J. La Haye, C.P. Moeller, A. Funahashi, T. Yamamoto, K. Hoshino, N. Suzuki, S.M. Wolfe, P.C. Efthimion, H. Toyama, and T. Roh, Nucl. Fusion 21:11, 1425 (1981).

2. R.P.H. Chang, M. Porkolab, and B. Grek, Phys. Rev. Lett. 28:4, 206 (1972); M. Okabayashi, K. Chen, and M. Porkolab, Phys. Rev. Lett. 31:18, 1113 (1973); M. Porkolab, V. Arunasalam, N.C. Luhmann, and J.P.M. Schmitt, Nucl. Fusion 16:2, 269 (1976).

3. R.M. Gilgenbach, M.E. Read, K.E. Hackett, R.F. Lucey, V.L. Granatstein, A.C. England, C.M. Loring, J.B. Wilgen, R.C. Isler, Y-K.M. Peng, K.H. Burrell, O.C. Eldridge, M.P. Hacker, P.W. King, A.G. Kulchar, M. Murakami, and R.K. Richards, Nucl. Fusion 21:3, 319 (1981).

4. W.A. Davis, Bull. Am. Phys. Soc. 26:7, 979 (1981); R.J. Colchin, Bull. Am. Phys. Soc. 26:7, 980 (1981).

5. A.T. Lin and Chih-Chien Lin, Phys. Rev. Lett. 47:2, 98 (1981).

6. M. Porkolab, Nucl. Fusion 18:3, 367 (1978); M. Porkolab and R.P.H. Chang, Rev. Mod. Phys. 50:4, 745 (1978).

7. M. Porkolab, Bull. Am. Phys. Soc. 26:7, 1023 (1981); M. Porkolab, Proc. 2nd Workshop on Hot Electron Ring Physics (December, 1981), (to be published).

8. B. Richards, D.S. Stone, A.S. Fisher, and G. Bekefi, Comments on Plasma Physics and Controlled Fusion 3, 117 (1978).

9. M.E. Read, R.M. Gilgenbach, B. Arfin, G. Bekefi, K. Burrell, K.R. Chu, O. Eldridge, A.C. England, V.L. Granatstein, K. Hackett, M. Hacker, H. Howe, B. Hui, R. Isler, P. King, A. Kulchar, E. Lazarus, M. Loring, M. Murakami, Y-K.M. Peng, R. Richards, and J.B. Wilgen, Proceedings 2nd Joint Grenoble-Varenna International Symposium on Heating in Toroidal Plasmas, EUR 7424 EN, p. 175 (September, 1980); M.E. Read, R.M. Gilgenbach, R.F. Lucey, Jr., K.R. Chu, A.T. Drobot, and V.L. Granatstein, IEEE Trans. on Microwave Theory and Techniques MTT-28, No. 8, 875 (1980).

10. We estimate that 70% of the incident power is coupled to the extraordinary mode.

11. A.J. Cohen and G. Bekefi, Phys. Fluids 14:17, 1512 (1971).

12. Decay into an electron Bernstein mode and ion acoustic wave has also been considered but does not affect the results presented here.

13. O. Eldridge, W. Namkung, and A.C. England, ORNL/TM-6052 (to be published); E. Ott, B. Hui, and K.R. Chu, Phys. Fluids 23:5, 1031 (1980).

14. J.J. Schuss, M. Porkolab, Y. Takase, D. Cope, S. Fairfax, M. Greenwald, D. Gwinn, I.H. Hutchinson, B. Kusse, E. Marmar,

D. Overskei, D. Pappas, R.R. Parker, L. Scaturro, J. West, and S. Wolfe, Nucl. Fusion 21:4, 427 (1981) and references therein.

FIGURE CAPTIONS

Fig. 1. Geometry of the electron cyclotron heating experiment, showing the electron cyclotron resonance surface $\omega_0=\omega_{ce}$, the upper-hybrid surface $\omega_0=\omega_{UH}$, and the electron cyclotron cutoff region (shown speckled).

Fig. 2. Radiation intensity measured with the Ka band spectrum analyzer showing (a) spectral power as a function of frequency; the first resonance on the left is at the reference (gyrotron) frequency $\omega_0/2\pi=35.08$GHz; and (b) the temporal variation of the radiation intensity at a difference frequency of 425MHz.

Fig. 3. Measurements of the radiation intensity obtained from (a) the Ka band detector and (b) from the RF probe, as a function of frequency.

Fig. 4. Peak radiation intensity obtained with the Ka band detector as a function of incident power from the gyrotron for line-averaged, central electron densities of ▲ $\bar{n}_e = 0.4\times10^{13}\text{cm}^{-3}$ and ● $\bar{n}_e=0.6\times10^{13}\text{cm}^{-3}$.

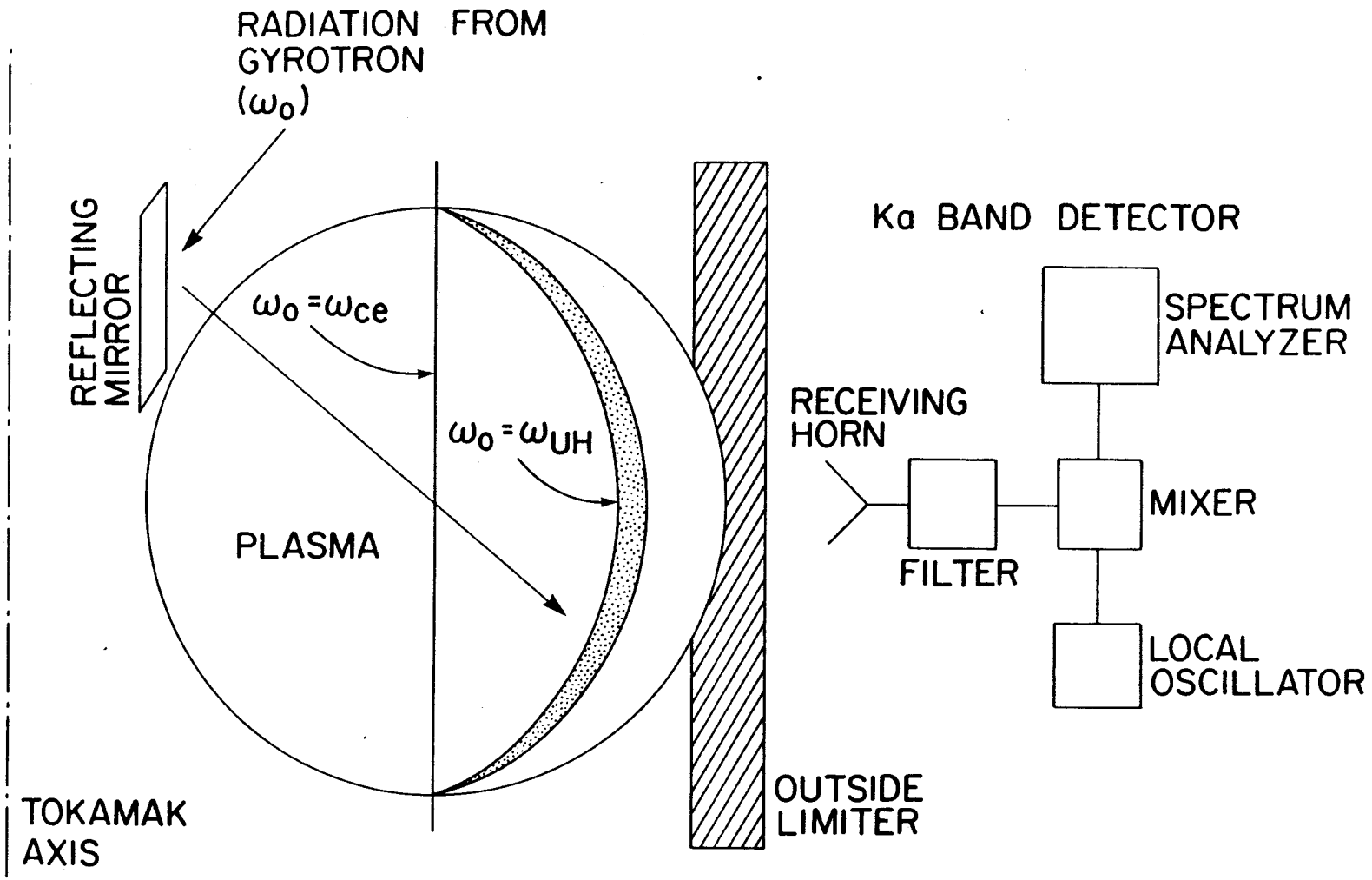

Fig. 1
McDermott, Bekefi, Porkolab

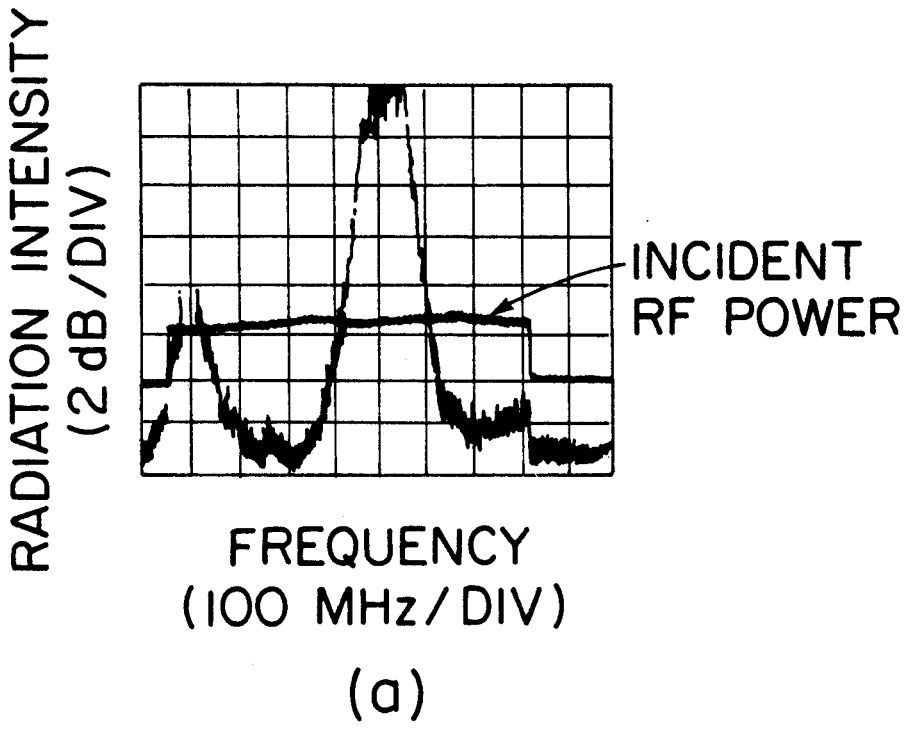

(a)

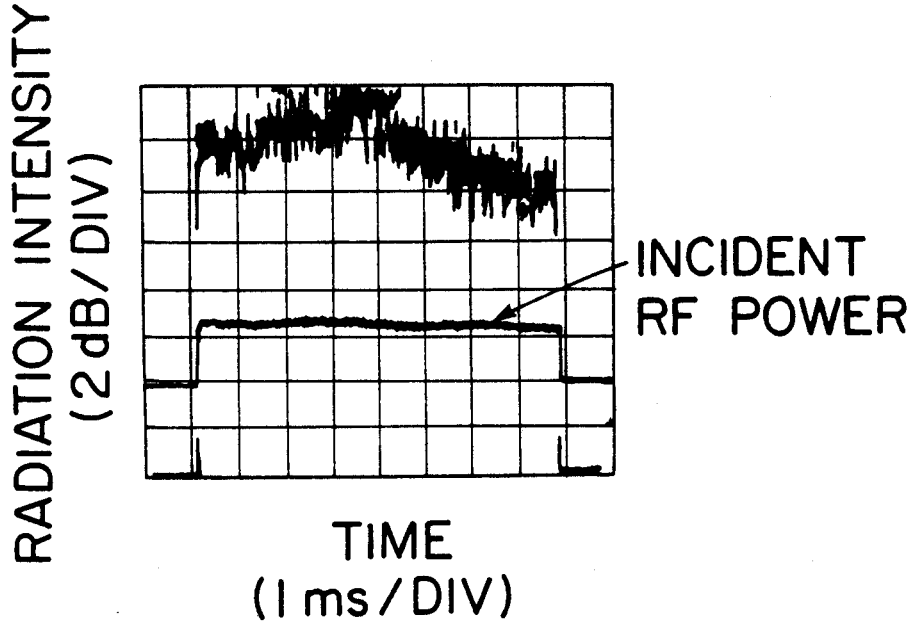

(b)

Fig. 2
McDermott, Bekefi, Porkolab

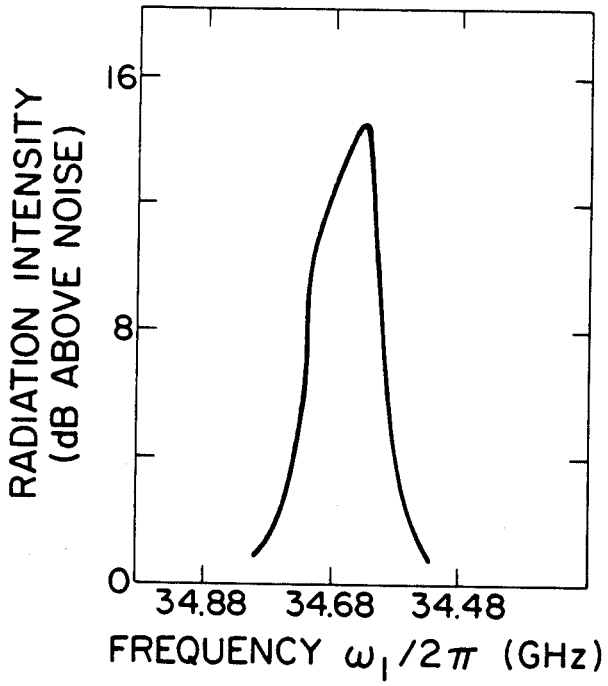

(a)

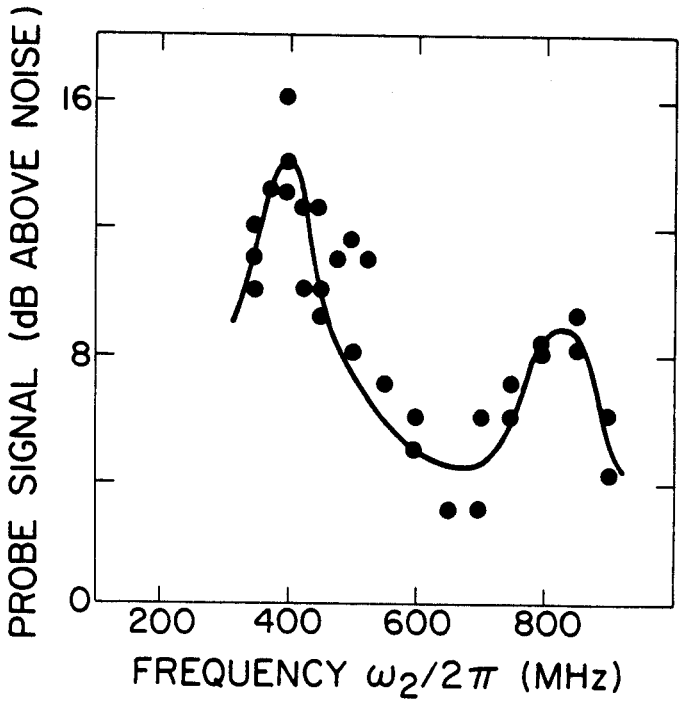

(b)

Fig. 3
McDermott, Bekefi, Porkolab

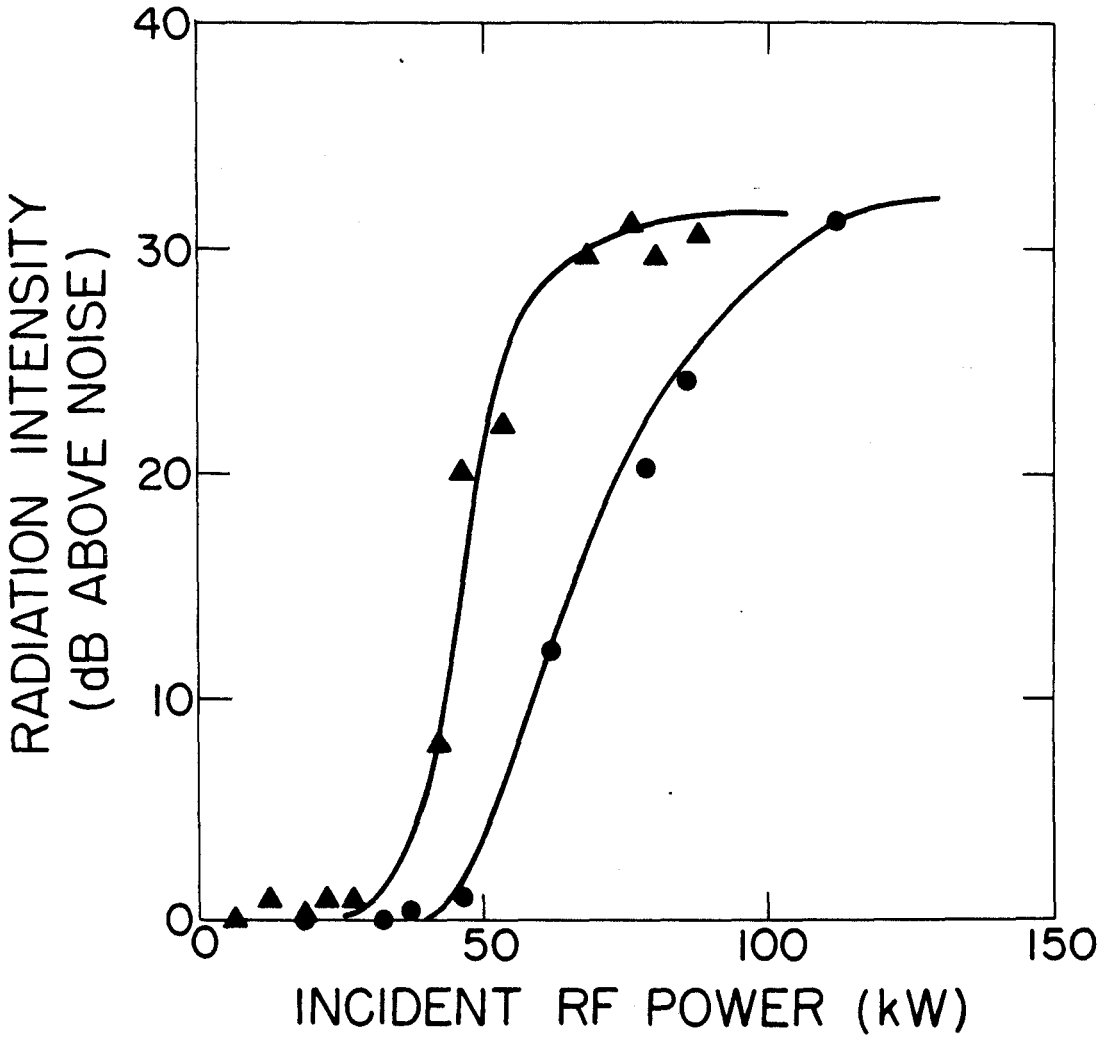

Fig. 4
McDermott, Bekefi, Porkolab